Monolayers of derivatized poly(L-lysine)-grafted poly(ethylene glycol) on metal oxides as a class of biomolecular interfaces

L. A. Ruiz-Taylor, T. L. Martin, F. G. Zaugg, K. Witte, P. Indermuhle, S. Nock, and P. Wagner*

Zyomyx, Inc., 3911 Trust Way, Hayward, CA 94545

Edited by Calvin F. Quate, Stanford University, Stanford, CA, and approved December 5, 2000 (received for review October 12, 2000)

We report on the design and characterization of a class of biomolecular interfaces based on derivatized poly(L-lysine)-grafted poly(ethylene glycol) copolymers adsorbed on negatively charged surfaces. As a model system, we synthesized biotin-derivatized poly(L-lysine)-grafted poly(ethylene glycol) copolymers, PLL-g-[(PEGm)$_{(1-x)}$ (PEG-biotin)$_x$], where *x* varies from 0 to 1. Monolayers were produced on titanium dioxide substrates and characterized by x-ray photoelectron spectroscopy. The specific biorecognition properties of these biotinylated surfaces were investigated with the use of radiolabeled streptavidin alone and within complex protein mixtures. The PLL-g-PEG-biotin monolayers specifically capture streptavidin, even from a complex protein mixture, while still preventing nonspecific adsorption of other proteins. This streptavidin layer can subsequently capture biotinylated proteins. Finally, with the use of microfluidic networks and protein arraying, we demonstrate the potential of this class of biomolecular interfaces for applications based on protein patterning.

Controlling immobilization of biomolecules on surfaces, while preventing nonspecific adsorption of unwanted species, has become an important goal for monitoring specific biointeractions and binding of biomolecules or cells. Indeed, in diagnostic assays, biomaterial devices, and surface-related bioanalytical applications, nonspecific protein binding can often be the obstacle to higher sensitivity, reproducibility, or implant integration. Therefore, in past decades, many immobilization strategies have been established. These include physisorption to solid organic or inorganic supports (noncovalent coupling occurs by electrostatic and van der Waals forces), noncovalent chemisorption, and covalent immobilization on organic thin films of different molecular organization.

Physisorption of biomolecules directly on the surface of inorganic substrate materials such as glass or organic coatings such as polymeric materials and adhesion layers (polylysine and nitrocellulose) probably constitutes the least technically challenging immobilization procedure. For instance, spotted microarrays of nucleic acids and, more recently, proteins are mostly based on physical adsorption (1). However, these methods suffer from some key limitations, such as their lack of control over the quantity and orientation of adsorbed biomolecules, and, hence, from lower reproducibility, lower interaction efficiencies, and high error rates. Moreover, additional passivation or blocking steps of the remaining sites are often required to limit the extent of nonspecific binding and protein denaturation. These are serious limitations for protein microarray applications.

Attempts to control the biomolecular density and orientation of biomolecules at the solid–liquid interface to obtain better reproducibility have been undertaken through various strategies of covalent and site-specific immobilization. These include mostly immobilization via organic thin films such as self-assembled alkanethiol and silane monolayers on noble metals and glass substrates, respectively. These monolayers often have rather simple functionalities such as carboxyl or amine terminations and need further activation to react with nucleophilic groups in the biomolecule (2–4). Monolayers formed from already bioreactive precursor molecules can also be created; biomolecules can then be directly and covalently bound to the surface in the absence of *in situ* transformations or coupling agents. Examples include *n*-hydroxysuccinimide-terminated self-assembled monolayers for amine coupling (5–7) or nitrilotriacetic acid/Ni^{2+} terminations for site-specific immobilization of oligohistidine tags (8, 9). These approaches constitute a clear improvement in the design of controlled interfacial architectures over physisorption techniques.

To date, wet and gas-phase silane monolayer formations are methods of choice for modifying glass and oxide surfaces (10–12). However, these monolayers are not always straightforward to prepare, because of a complex condensation process at the interface and result very often in unpredictable molecular densities of exposed ω-functionalities. Therefore appropriate choice of the silane coupling chemistry and careful control of the reaction conditions (13, 14) are mandatory. Other types of monolayers on oxides have yet to be investigated to avoid these disadvantages. These include organic phosphoric or phosphonic acid derivatives on metal oxides (15, 16) and a class of monomolecular layers of poly(L-lysine)-grafted-poly(ethylene glycol) (or PLL-g-PEG) copolymers adsorbed on negatively charged surfaces. The latter has been found to spontaneously adsorb from aqueous solution onto any surface that is negatively charged under physiological conditions (among these are glass and metal oxides such as SiO_2, TiO_2, Nb_2O_5, etc.) with its polycationic PLL backbone strongly interacting with the surface and the PEG side chains extending toward the aqueous solution. As a result, the PLL-g-PEG forms a monolayer, which is thus very different from the ill-defined architecture of polylysine dip coatings. Furthermore, PEG compounds are known for limiting nonspecific protein binding (17–21), and, as a result, the PLL-g-PEG monolayer reduces significantly the adsorption of proteins from blood serum, as reported by Kenausis *et al.* (22).

Our aim is to extend the basic PLL-g-PEG system and convert it from a protein-resistant surface to an interface with specific bioreactivity, while maintaining its protein resistance characteristic. Here we present a PLL-g-PEG system with additional reactive sites for the specific and stable immobilization of biomolecules (such as proteins, DNA/RNA, etc.). Such a system (PLL-g-[$(PEG)_{1-x}$(PEG-X)$_x$]) has numerous advantages, among which are the spontaneous adsorption property of the polymer and its efficiency in repelling nonspecific protein binding while still providing PEG tethered functional/active sites for specific biomolecular recognition (see Fig. 1). Dilution of the functional groups occurs directly in solution when the PEG side chains are

This paper was submitted directly (Track II) to the PNAS office.

Abbreviations: PLL, poly(L-lysine); PEG, poly(ethylene glycol); PEGm, methoxy-PEG; XPS, x-ray photoelectron spectroscopy; PDMS, poly(dimethylsiloxane); S-FITC, fluorescein-labeled streptavidin; PE, phycoerythrin; b-PE, biotinylated PE.

*To whom reprint requests should be addressed. E-mail: peter.wagner@zyomyx.com.

The publication costs of this article were defrayed in part by page charge payment. This article must therefore be hereby marked "*advertisement*" in accordance with 18 U.S.C. §1734 solely to indicate this fact.

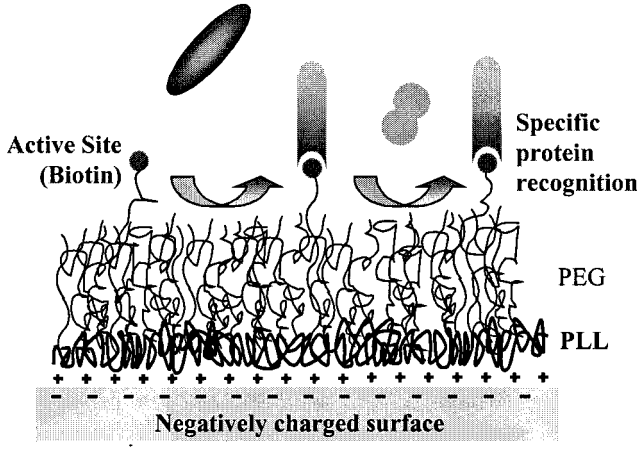

Fig. 1. Schematic organization of the PLL-g-[$(PEGm)_{1-x}$(PEG-site)$_x$] interface.

grafted to the PLL. This allows us to control and limit the surface density of reactive sites and therefore the surface density of immobilized proteins. In addition, the use of PEG tethers for biomolecular immobilization has been reported to minimize loss of protein activity (23).

This paper describes the synthesis and characterization of a biotin-derivatized poly(L-lysine)-grafted poly(ethylene glycol), PLL-g-[$(PEGm)_{1-x}$(PEG-biotin)$_x$], with x ranging from 0 to 1. Derivatization of the polymer with biotin provides a suitable model system and allows the use of a large variety of streptavidin-labeled reagents for more in-depth studies. The usefulness of this approach to protein microarraying will be demonstrated with two examples: (*i*) a one-dimensional channel type pattern and (*ii*) a two-dimensional array of fluorescent protein exhibiting feature sizes of 50 μm.

Materials and Methods

Synthesis of PLL-g-[$(PEGm)_{1-x}$(PEG-biotin)$_x$] Copolymers. Synthesis of biotin-derivatized PLL-g-PEG copolymers was adapted from the protocol described by Elbert and Hubbell (24) for the synthesis of methoxy-terminated PLL-g-PEG. Poly(L-lysine) (PLL) (15–30 kDa; Sigma) was dissolved in 50 mM sodium tetraborate buffer (pH 8.5) at a concentration of 40 mg/ml. The solution was filter-sterilized. Solid *n*-hydroxysuccinimidyl ester of methoxy-PEG (PEGm) proprionic acid (2 kDa; Shearwater Polymers, Huntsville, AL) and α-biotin-ω-hydroxysuccinimidyl ester of PEG-carbonate (3.4 kDa; Shearwater Polymers) were added to the dissolved PLL solution in the desired stoichiometric ratio under vigorous stirring. The reaction was allowed to proceed for 6 h at room temperature, after which the reaction mixture was dialyzed (Spectra/Por, molecular weight cut off 15 kDa; Spectrum, Rancho Dominguez, CA) against PBS at pH 7.4 for 24 h and subsequently against deionized water for 24 h. The dialyzed solution was lyophilized for 48 h and stored under nitrogen at −25°C.

Seven PLL-g-[$(PEGm)_{1-x}$(PEG-biotin)$_x$] copolymers (also referred to as PLL-g-PEG-Bx%) were synthesized with biotin contents corresponding to x (%) = 0, 1, 10, 20, 30, 50, and 100. The grafting ratio (the ratio of the number of lysine units to the number of grafted PEG chains) was kept at a constant value of 3.5:1 to ensure a PEG density that is sufficient to guarantee both nonspecific protein binding resistance and a sufficient number of protonated amines for surface binding (22). In other words, the total number of PEG side chains (whether biotin- or methoxy-terminated) is kept constant for a given number of lysine units, and the number of biotin-terminated PEG side chains is then a fraction (x) of the total number of PEG chains. Fig. 2 represents a schematic of the copolymer structure.

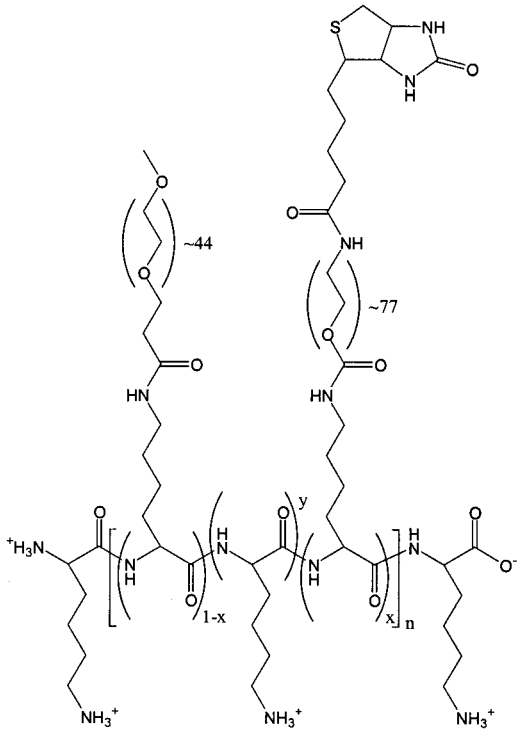

Fig. 2. Schematic structure of the PLL-g-[$(PEGm)_{1-x}$(PEG-biotin)$_x$] copolymers; x is the fraction of the derivatized PEG side chains, y is the total number of free lysine units per PEG side chain, and n is the total number of lysine units.

^{1}HNMR in D_2O, δ [ppm] = 1.33–1.60 (Lys, CH_2), 2.15 (biotin, -CH_2 C(O)N-), 2.4 (coupled PEGm, -CH_2-C(O)-NH), 2.65 (biotin, -S-CH), 2.88 (free Lys, -N-CH_2), 3.06 (PEGm activated Lys, C(O)-NH-CH_2-), 3.25 (PEGm, -O-CH_3), 3.55 (PEGm, CH_2-O-), 4.18 (Lys, N-CH-C(O)-), 4.29 and 4.45 (biotin, 2 bridgehead CH).

The biotin content of the copolymers was determined with the use of 2-(4′-hydroxyazobenzene) benzoic acid (ImmunoPure HABA; Pierce) via UV/visual spectroscopy at 500 nm. Results are reported per mg copolymer: PLL-g-PEGm (0 nmol); PLL-g-PEG-B1% (3 nmol); -B10% (37 nmol); -B20% (62 nmol); -B30% (94 nmol); -B50% (131 nmol); -B100% (197 nmol).

PLL-g-[$(PEGm)_{1-x}$(PEG-biotin)$_x$] copolymers were dissolved in 10 mM Hepes buffer (pH 7.4) at a concentration of 1 mg/ml unless otherwise mentioned. All solutions were filter-sterilized with 0.2-μm cellulose acetate sterile filters and stored at 4°C until use.

Monolayer Formation and Surface Reactions. Substrates consisted of a 20-nm-thick titanium dioxide (TiO_2) layer deposited on Si (100) wafers with a 250-nm layer of thermally grown SiO_2 (Silicon Quest International, Santa Clara, CA). The wafers were cut into 1 × 1 cm^2 pieces and cleaned immediately before monolayer formation by exposure to oxygen plasma for 30 s at 200 W. These substrates were also used for microfluidic protein patterning experiments.

PLL-g-[$(PEGm)_{1-x}$(PEG-biotin)$_x$] monolayer formation. Under class 100 conditions, a 60-μl drop of the prepared copolymer solution was deposited on a piece of parafilm. The sample was placed on the droplet with its TiO_2 surface facing the drop and covered with a Petri dish. Triplicate samples were incubated for 30 min. They were then extensively rinsed with 40–50 ml of PBS (pH 7.4). Samples for surface analysis were additionally rinsed

with 40–50 ml of nanopure water and dried under a nitrogen stream.

Protein incubation and radiometry. Streptavidin (S) (60 kDa, from *Streptomyces avidinii*, recombinantly expressed in *Escherichia coli*; Sigma) was dissolved in PBS (pH 7.4). ^{125}I-radiolabeled streptavidin (S*, ≈38.5 μCi/μg; Amersham Pharmacia) was diluted with nonlabeled streptavidin (resulting specific activity of ≈30–40 nCi/μg). The total streptavidin concentration of the S*/S mixture was determined by UV/visual spectroscopy at 280 nm, with an extinction coefficient of 57,000 $M^{-1}\cdot cm^{-1}$ (25). ^{125}I-radiolabeled mouse mAb AU1 (IgG_3/κ; Covance, Richmond, CA) was diluted with nonlabeled AU1 in PBS (resulting specific activity of ≈1.2 μCi/μg). A highly concentrated protein mixture was prepared as follows: *E. coli* strain (XL1-Blue) was grown overnight in 2 × YT broth (Bio 101, Carlsbad, CA) and sonicated to lyse the cells. The mixture was then spun down (20,000 rpm for 45–60 min), and the cytoplasmic fraction was collected. Native biotinylated species were further removed from the cytoplasmic fraction by affinity purification over avidin immobilized on 6% crosslinked beaded agarose (Pierce). Protein concentrations were determined by UV/visual spectroscopy at 750 nm by the Lowry procedure with a BSA standard.

Protein incubation on the PLL-g-PEG(-biotin) monolayers was carried out by the procedure described above. Proteins were usually incubated for 1 h, which was sufficient to reach saturation. Protein standards were prepared with 2.5, 5, 25, and 50× dilutions. Samples and standards were exposed for 3–15 h against a storage phosphor screen (Molecular Dynamics), and the screen was then scanned with a PhosphorImager (STORM820, IMAGEQUANT software; Molecular Dynamics).

X-Ray Photoelectron Spectroscopy (XPS). XPS analyses were performed with a Quantum 2000 Scanning ESCA Microprobe (Physical Electronics, PHI, Eden Prairie, MN) equipped with a spherical capacitor energy analyzer used in the fixed analyzer transmission mode. The base pressure of the system was less than 10^{-9} Torr, and spectra were typically acquired at a pressure below 5×10^{-9} Torr with a monochromatized Al K_α source operating at 100 W, with a beam diameter of 100 μm. Sample charge-up was compensated for with a flux of low-energy electrons combined with a small current of low-energy positive ions (26). Under these conditions, the energy resolution for detailed scans [full width at half-maximum measured on silver $Ag(3d_{5/2})$] was 0.8 eV. Spectra were referenced to the substrate $Ti(2p_{3/2})$ signal at 458.5 eV. Data were analyzed with a least-squares fit routine after iterative Shirley background subtraction. Measured intensities derived from peak areas were corrected by their respective photoionization cross section corresponding to PHI sensitivity factors (27) as well as for transmission function, angular distribution factor, and asymmetry factor (28, 29). Spectra were fitted with MULTIPACK software (version 6.1A, PHI), with the use of the sum of a 95% Gaussian and 5% Lorentzian function.

Protein Microfluidic Patterning. A silicon master with 20-μm-deep channels of different widths ranging from 5 to 200 μm was fabricated by standard photolithographic protocols, including a deep reactive ion etching step, and was silanized from gas phase with hexamethyldisilazane. An elastomeric microfluidic channel array was prepared from poly(dimethylsiloxane) (PDMS) and applied as described (30).

Patterning of surfaces was performed as follows. The PDMS channels were first positioned on the TiO_2 surface. Approximately 25 μl of either PLL-g-PEGm or PLL-g-PEG-B20% solution (0.25 mg/ml) was placed at one end of the openings of the channels. The solution then passed through the channels via capillary forces. The surface was placed in a humidity chamber and allowed to sit at room temperature to ensure complete coverage of the surface by the PLL-g-PEG(-biotin) copolymer. After 1 h, the channels were rinsed with Hepes buffer. The PDMS was then removed and the surface immediately rinsed with 40 ml of Hepes. The second step consisted of backfilling the polymer-free areas that were originally in contact with the PDMS device with the opposite PLL-g-PEG(-biotin) solution, which was accomplished by placing the sample upside down on a 60-μl drop of the copolymer solution. After 30 min of incubation, the surface was rinsed again with 40 ml of PBS (pH 7.4). In the third step, the modified surface was incubated for 1 h with either streptavidin (233 nM in PBS, pH 7.4; Sigma), fluorescein-labeled streptavidin (S-FITC) (233 nM in PBS; Sigma), or S-FITC (233 nM in PBS) diluted into a 1,000× molar excess of free biotin. Samples incubated with S-FITC were then rinsed extensively with 40 ml of PBS followed by 30 ml of nanopure water. Samples incubated with unlabeled streptavidin were further exposed to 1 μM PBS solutions of the biotinylated or nonbiotinylated fluorescent protein R-phycoerythrin (b-PE or PE; Molecular Probes). After 1 h of incubation, samples were rinsed extensively with 40 ml of PBS and 30 ml of nanopure water. Finally, all samples were examined by fluorescence microscopy [Zeiss Axioplan2 microscope with a 20× objective lens, a Zeiss 100-W mercury arc lamp, and High Q fluorescein and rhodamine filter sets (Chroma Technology, Brattleboro, VT)].

Protein Microarraying. A silicon substrate covered with 20 nm of TiO_2 was incubated with a solution of PLL-g-PEG-B30% (1 mg/ml) for 1 h at room temperature. The chip was then rinsed thoroughly with 50 ml of PBS (pH 7.4), incubated with streptavidin (1.7 μM in PBS) for 30 min at room temperature, and rinsed again with 50 ml of PBS followed by 50 ml of nanopure water. After removal of excess water with a stream of nitrogen, the chip was stored briefly under 100% humidity before protein arraying.

A solution containing the biotinylated fluorescent protein b-PE at a concentration of 1 μM in PBS was dispensed in a 40 × 40 array format onto the activated chip with the use of an in-house-built microarrayer. After 10 min of incubation, the chip was then rinsed with 50 ml of PBS followed by 25 ml of nanopure water and immediately scanned with a confocal fluorescence scanner (ScanArray 5000; GSI Lumonics, Billerica, MA) at 543-nm excitation and 578-nm emission.

Results and Discussion

Monolayer Characterization. XPS has been used to characterize PLL-g-$[(PEGm)_{1-x}(PEG\text{-}biotin)_x]$ (x = 0 to 1) monolayers adsorbed on titanium dioxide substrates with respect to basic elemental concentrations and chemical states. An in-depth investigation of the properties and organization of the different PLL-g-PEG(-biotin) interfaces, including their interactions with different proteins, has been completed and will be described in a separate contribution.

Fig. 3*a* shows an example of the XPS survey spectrum of PLL-g-PEG-B20% on titanium dioxide. The main contributions are oxygen (O_{1s}), carbon (C_{1s}), and nitrogen (N_{1s}) arising from the PLL-g-PEG-biotin overlayer, and titanium (Ti_{2p}) and oxygen from the substrate. Sulfur (S_{2p}) from the biotin endgroup was below the detection limits of the spectrometer and therefore could not be detected. Nevertheless, the strong signals of the substrate peaks suggest that the PLL-g-PEG(-biotin) overlayer is indeed monomolecular in nature. Fig. 3*b* displays the deconvolution of the most relevant high-energy resolution scan, namely oxygen (O_{1s}), for the same surface. Two main contributions can clearly be identified. The lowest binding energy component at 530 eV corresponds to the oxygen of the TiO_2 substrate, and the highest binding energy component at 533 eV corresponds to the ether oxygen, which exclusively originates from the PEG side

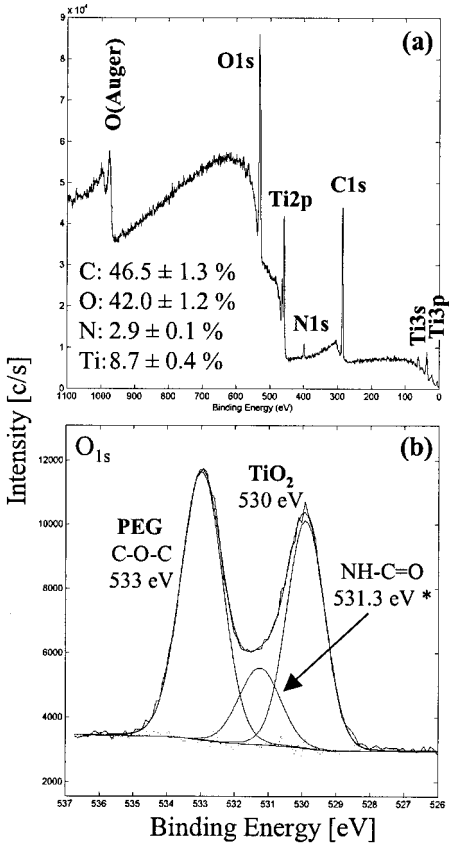

Fig. 3. XPS survey (*a*) and oxygen O_{1s} high-energy resolution scans (*b*) of the PLL-g-PEG-B20% copolymer on TiO_2 (the emission angle is 20°). *Urea and urethane contributions do not differ significantly in binding energy from amide contributions to be deconvoluted separately.

chains of the copolymer. A third contribution at 531.3 eV can be resolved by deconvolution. The latter essentially arises from the oxygen of the amide bonds of the PLL backbone, the ω-terminations of the PEG chains, and the biotin (see Fig. 2).

By deconvoluting the oxygen signals, it is possible to estimate the substrate coverage by the PLL-g-PEG(-biotin) monolayer. The PEG/TiO_2 intensity ratio of the oxygen peaks provides an indirect measurement of the biotin surface concentration of the monolayers. Indeed, a higher molar ratio of the biotinylated to nonbiotinylated PEG side chains results in a larger amount of the longer biotin-PEGs (77 units) and a smaller amount of the shorter methoxy-PEGs (44 units). As a consequence, an increased PEG coverage results in a stronger attenuation of the substrate Ti and O_{TiO2} peak intensities (data not shown).

Biomolecular Recognition Characteristics. Biomolecular recognition properties of the monolayers were investigated via radiometry and XPS to assess the specificity of the binding event toward streptavidin and the ability of the system to reduce nonspecific binding.

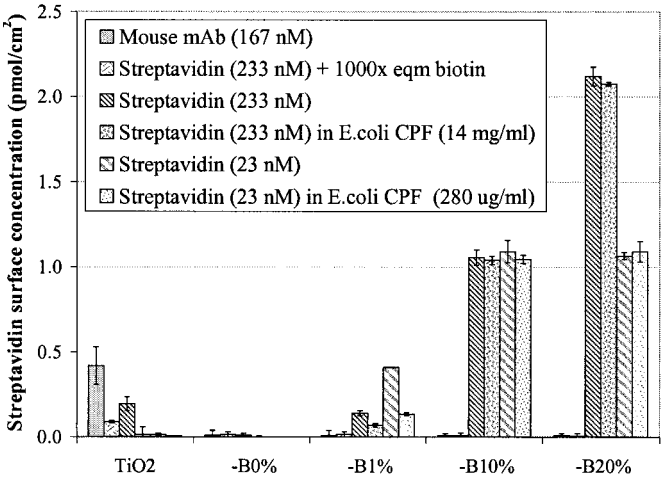

Fig. 4. Recognition properties of PLL-g-[$(PEGm)_{1-x}$(PEG-biotin)$_x$] copolymers with $x = 0$ to 0.2. Surface concentrations of the mouse mAb incubated in PBS and streptavidin incubated in either PBS alone, previously mixed with free biotin, or incubated in PBS containing a high protein concentration from the *E. coli* cytoplasmic fraction (CPF).

We first investigated the nonspecific protein repelling characteristics of the monolayers. Table 1 reports the relative atomic concentrations determined by XPS for the PLL-g-PEG-B20% monolayer after protein incubation. As a comparison, we also report the atomic concentrations measured for a TiO_2 surface incubated with either streptavidin or an *E. coli* cytoplasmic fraction. The atomic concentrations of the streptavidin-incubated bare TiO_2 samples are almost comparable to those measured on the plain TiO_2 after oxygen plasma cleaning (Table 1), thus suggesting that only a minute amount of streptavidin binds to the bare TiO_2 surface. This lack of binding of streptavidin to TiO_2 is most likely due to the isoelectric point of the protein (around 5–6) (31), which renders it slightly negatively charged at pH 7.4 and may build up repulsive interactions with the TiO_2 surface. In contrast, uncoated TiO_2 samples incubated with the *E. coli* cytoplasmic fraction show increased carbon and nitrogen amounts compared with the bare substrate, suggesting that proteins have irreversibly bound to the TiO_2 surface. Comparison of the results obtained for the PLL-g-PEG-B20% samples shows that incubation of the monolayers with either PBS or an *E. coli* cytoplasmic fraction does not give way to significantly different surface atomic concentrations. Hence the amount of protein that binds nonspecifically and irreversibly to the PLL-g-PEG-B20%-modified TiO_2 surfaces is not significant (within the detection limits of the XPS technique). However, when the PLL-g-PEG-B20% monolayer is incubated with

Table 1. Relative atomic concentration (± SD) of the TiO_2 surfaces either bare or modified with PLL-g-PEG-B20% monolayers and incubated with PBS, streptavidin (200 nM), or *E. coli* cytoplasmic fraction (1.3 mg/ml) (emission angle 20°)

	Incubation	C, %	O, %	N, %	Ti, %
TiO_2	—	18.7 ± 1.5	57.7 ± 0.4	0.9 ± 0.1	22.7 ± 0.9
TiO_2	Streptavidin	20.1 ± 1.0	57.5 ± 0.6	1.3 ± 0.8	21.1 ± 1.1
TiO_2	*E. coli*	51.3 ± 0.0	29.7 ± 0.6	13.1 ± 0.3	5.9 ± 0.3
PLL-g-PEG-B20%	PBS	46.5 ± 1.3	42.0 ± 1.2	2.8 ± 0.1	8.7 ± 0.4
PLL-g-PEG-B20%	Streptavidin	57.6 ± 0.6	30.5 ± 0.3	8.5 ± 0.2	3.4 ± 0.4
PLL-g-PEG-B20%	*E. coli*	46.0 ± 0.4	41.9 ± 0.2	3.0 ± 0.1	9.1 ± 0.1

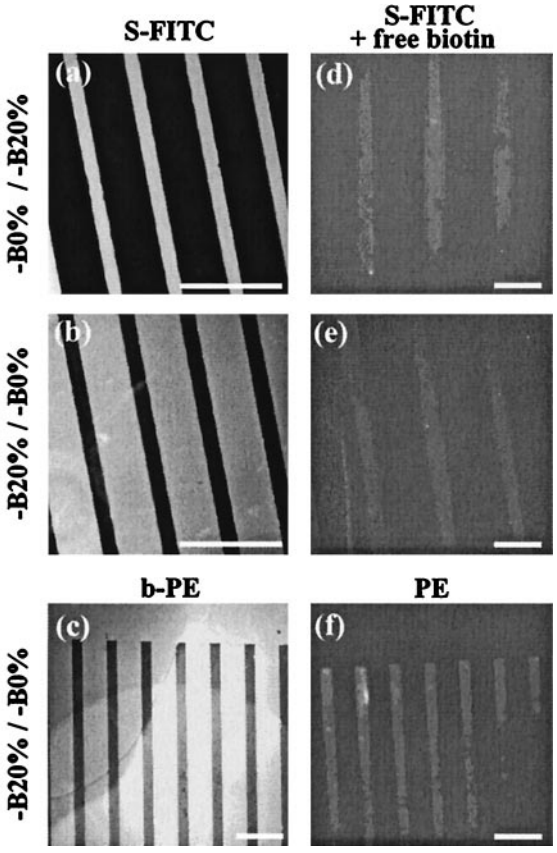

Fig. 5. Fluorescence microscopy images of streptavidin-FITC bound to patterned PLL-g-PEG(-biotin) surfaces. In *a* and *b*, the patterned surface was incubated with S-FITC; in *d* and *e*, it was incubated with S-FITC diluted in a 1000× molar excess of free biotin. Contrast and brightness had to be adjusted. In *c* and *f*, the patterned surface was incubated first with streptavidin and then with biotinylated phycoerythrin (b-PE) (*c*) or phycoerythrin (PE) (*f*). (The scale bar is 100 μm.)

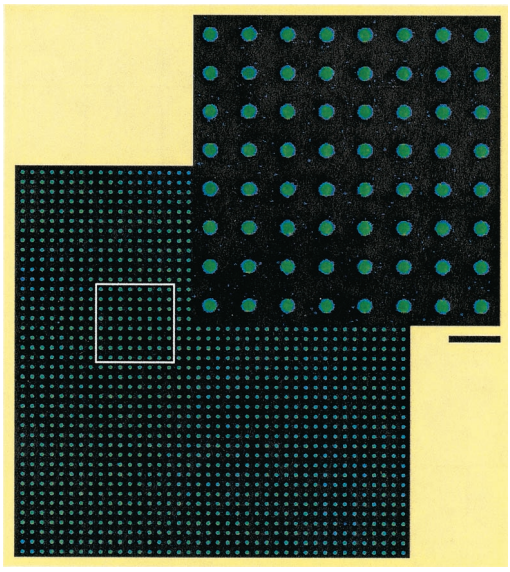

Fig. 6. Fluorescence picture of a 40 × 40 microarray of biotin-phycoerythrin dispensed on streptavidin-incubated PLL-g-PEG-B30%. Each spot is 50 μm in diameter. (The scale bar is 200 μm.)

streptavidin, there is a dramatic increase in both carbon and nitrogen amounts, which shows that streptavidin is bound to the surface. Correspondingly, oxygen and titanium amounts decrease because of attenuation of the substrate signal intensities by the additional protein layer.

Fig. 4 shows the amount of proteins bound to PLL-g-PEG-(-biotin) monolayers of increasing biotin content (from -B0% to -B20%) under a variety of conditions. The ability of the PLL-g-PEG(-biotin) surfaces to prevent nonspecific adsorption was also tested against a ^{125}I-labeled mouse mAb. As shown, the antibody adsorbs slightly (≈0.5 pmol/cm^2) to the bare TiO_2 surface. However, as soon as the oxide is modified with the PLL-g-PEG monolayer, whether it contains biotin or not, no mAb can be detected at the surface of the sample, thus showing that the mAb was repelled by the PLL-g-PEG(-biotin) monolayers. Finally, the specificity of the streptavidin binding was determined in a competitive binding assay, with streptavidin diluted in a 1,000-fold molar excess of free biotin. This dilution in biotin led to saturation of the specific binding sites of streptavidin before interaction with the PLL-g-PEG(-biotin) surfaces. As expected, no streptavidin could be detected on any of the surfaces, including those with higher biotin contents (-B30% to -B100%; data not shown), hence demonstrating that the binding was entirely specific.

Furthermore, as displayed in Fig. 4, streptavidin binding to the bare TiO_2 is limited (≈0.2 pmol/cm^2), in agreement with our XPS measurements. On the PLL-g-PEGm (-B0%) modified surface, no streptavidin can be detected. However, as soon as biotin is present at the surface, streptavidin adsorbs specifically, and its surface concentration increases linearly with the biotin surface concentration, for the biotin range investigated (-B0% to -B100%). When streptavidin is spiked into a protein mixture prepared from an *E. coli* cytoplasmic fraction (in PBS) with a high mass ratio and the mixture is then exposed to the PLL-g-PEG(-biotin) monolayers, the streptavidin surface concentration matches the surface concentration of streptavidin incubated from PBS alone. This consistency in the streptavidin surface concentration shows that the recognition of streptavidin by the surface is not affected by the presence of other proteins, even at high concentrations. Hence not only are the PLL-g-PEG(-biotin) monolayers able to specifically fish streptavidin out of a complex protein mixture; they also efficiently prevent the nonspecific adsorption of other proteins (which would otherwise block surface sites). Finally, when the incubating solution is depleted in streptavidin by a factor of 10 (the streptavidin concentration is 23 nM in solution), recognition still occurs and similar surface concentration levels are reached on the PLL-g-PEG-B10% monolayer regardless of the presence of *E. coli* proteins. In the case of the PLL-g-PEG-B20% monolayer, there is not enough streptavidin available in solution to reach saturation of the monolayer. Only half of the saturation concentration is achieved, which is equivalent to the full binding capacity of the PLL-g-PEG-B10% monolayer. Again, whether streptavidin is in a PBS solution or in a complex protein mixture, the recognition level is not affected, because identical surface concentrations can be determined. These experiments show that PLL-g-PEG(-biotin) monolayers can promote the specific recognition of target biomolecules such as streptavidin, while still efficiently preventing nonspecific adsorption of other proteins. This dual function is an important feature for biotin-based bioanalytical applications with samples of complex nature.

Protein Patterning. In a first example, we have used a PDMS mold with longitudinal channels to demonstrate the feasibility of using the PLL-g-PEG(-biotin) system to create protein patterns on TiO_2. Fluorescence microscopy was used to identify the binding location of S-FITC and R-phycoerythrin (PE) adsorbed on the PLL-g-PEGm/PLL-g-PEG-B20% patterned surfaces. The re-

sults of different experiments are displayed in Fig. 5. The wider bands correspond to the location of the channels filled by the copolymer solution first. The narrower bands correspond to the channel wall locations, namely the areas of the TiO_2 surface blocked by the PDMS elastomer and later exposed to the corresponding copolymer solution used for backfilling. The bright regions indicate the position of the S-FITC or the PE proteins. The pattern displayed in Fig. 5*a* was generated by first filling the channels with the PLL-g-PEGm (-B0%) solution and backfilling with the PLL-g-PEG-B20% solution. The pattern shown in Fig. 5*b* was generated with the use of a reversed loading; that is, channels were filled with PLL-g-PEG-B20%, and PLL-g-PEGm was used as backfill. One can note the sharp contrast between the bright areas where S-FITC is adsorbed and the dark regions where it is not. It is evident from the images that there is no lateral diffusion of either solution into neighboring areas and, therefore, no cross-contamination of the two copolymers on the TiO_2 surface. In addition, the pattern shown in Fig. 5*b* is the negative image of the pattern in Fig. 5*a*, and the bright areas are always located on the PLL-g-PEG-B20% regions. Hence the binding of streptavidin is specific to the areas of the surface that contain biotin and is inhibited on the PLL-g-PEGm areas. If the TiO_2 surface is now patterned like the sample in Fig. 5*b* but incubated first with streptavidin and then exposed to the biotinylated fluorescent protein b-PE, the resulting fluorescent pattern shown in Fig. 5*c* is observed. As can be seen with sharp contrast, b-PE binding occurs selectively on the PLL-g-PEG-B20%/streptavidin areas and is limited on the PLL-g-PEGm regions.

Patterns presented in Fig. 5 *d* and *e* were generated following the same order as for Fig. 5 *a* and *b*, respectively, but were incubated with S-FITC previously diluted in a 1,000-fold molar excess of free biotin, in a competitive binding assay. In comparison to Fig. 5 *a* and *b*, there is now little contrast between the different areas, indicating that hardly any streptavidin is binding to the surface and thus demonstrating that streptavidin binding to the copolymer is biotin specific. Similarly, when the sample shown in Fig. 5*c* is exposed to nonbiotinylated PE (Fig. 5*f*) instead of b-PE, no binding is observed on the PLL-g-PEG-B20% areas, thus showing that the secondary binding of b-PE on the sample is now streptavidin specific and that PE nonspecific binding is limited on the PLL-g-PEG(-biotin) monolayers.

Nevertheless, one can note in Fig. 5 *d–f* that the narrower bands corresponding to the areas of the sample that were in contact with the PDMS elastomer are slightly brighter. This result indicates that some S-FITC or nonbiotinylated PE adsorbs to these areas, independently of the location of the PLL-g-PEG-B20% copolymer. Although limited, some nonspecific physisorption of the proteins occurs on those regions, which is due solely to contamination of the TiO_2 by PDMS. This contamination is a well-known problem and a real limitation when such a material is used in protein patterning applications. Similar nonspecific binding of streptavidin is likely occurring in Fig. 5 *a–c* but is not detected because of the high contrast between the PLL-g-PEGm and PLL-g-PEG-B20% regions.

Finally, as a second example, Fig. 6 displays an array of 40 × 40 spots of 50-μm diameter of the fluorescent b-PE protein specifically bound to streptavidin on PLL-g-PEG-B30%. Of note is the sharp contrast between the b-PE spots compared with the background of the chip. This example also illustrates the potential of the PLL-g-PEG(-biotin) monolayers in protein micropatterning applications.

Conclusions

The aim of this project was to develop a class of interfaces based on biotin-derivatized poly(L-lysine)-grafted poly(ethylene glycol) copolymers, investigate its biomolecular binding characteristics and assess its behavior in protein patterning applications. We have demonstrated that the monolayers generated on TiO_2 are resistant to nonspecific protein binding and that streptavidin binding to these surfaces is entirely specific. Furthermore, the streptavidin recognition event is not affected by the presence of other proteins, even at high concentrations, and PLL-g-PEG-biotin monolayers can specifically capture streptavidin from a complex protein mixture while still preventing nonspecific adsorption of other proteins. We also demonstrated the feasibility of using the PLL-g-PEG(-biotin) system to generate selective micropatterns of specifically adsorbed and active proteins via microfluidic networks or protein arraying. In both cases, nonspecific binding has been mostly suppressed. These characteristics constitute valuable assets for building specific monomolecular interfaces for biosensing and protein patterning applications.

We acknowledge M. Heidecker, P. Lin, B. Muehlbauer, and N. Tolani for their contribution to the work.

1. Schena, M., Shalon, D., Davis, R. W. & Brown, P. O. (1995) *Science* **270,** 467–470.
2. Xiao, S. J., Textor, M. & Spencer, N. D. (1998) *Langmuir* **14,** 5507–5516.
3. Rogers, K. R. & Mulchandani, A., eds. (1998) *Affinity Biosensors: Techniques and Protocols* (Humana, Totowa, NJ).
4. Hermanson, G. T., Mallia, A. K. & Smith, P. K. (1992) *Immobilized Affinity Ligand Techniques* (Academic, San Diego).
5. Wagner, P., Zaugg, F., Kernen, P., Hegner, M. & Semenza, G. (1996) *J. Vacuum Sci. Technol.* **B14,** 1466–1471.
6. Wagner, P., Hegner, M., Kernen, P., Zaugg, F. & Semenza, G. (1996) *Biophys. J.* **70,** 2052–2066.
7. Zaugg, F. G., Wagner, P., Kernen, P., Vinckier, A., Groscurth, P., Spencer, N. D. & Semenza, G. (1999) *J. Materials Sci. Materials Med.* **10,** 1–9.
8. Sigal, G. B., Bamdad, C., Barberis, A., Strominger, J. & Whitesides, G. M. (1996) *Anal. Chem.* **68,** 490–497.
9. Kröger, D., Liley, M., Schiweck, W., Skerra, A. & Vogel, H. (1999) *Biosens. Bioelectron.* **14,** 155–161.
10. Weetall, H. H. (1993) *Appl. Biochem. Biotechnol.* **41,** 157–188.
11. Plueddemann, E. P., ed. (1991) *Silane Coupling Agents* (Plenum, New York).
12. Ulman, A. (1991) *An Introduction to Organic Thin Films: From Langmuir-Blodgett to Self-Assembly* (Academic, San Diego).
13. Parikh, A. N., Allara, D. L., Azouz, I. B. & Rondelez, F. (1994) *J. Phys. Chem.* **98,** 7577–7590.
14. Combes, J. R., White, L. D. & Tripp, C. P. (1999) *Langmuir* **15,** 7870–7875.
15. Brovelli, D., Hähner, G., Ruiz, L., Hofer, R., Kraus, G., Waldner, A., Schlösser, J., Oroszlan, P., Ehrat, M. & Spencer, N. D. (1999) *Langmuir* **15,** 4324–4327.
16. Textor, M., Ruiz, L., Hofer, R., Rossi, A., Feldman, K., Hähner, G. & Spencer, N. D. (2000) *Langmuir* **16,** 3257–3271.
17. Pale-Grosdemange, C., Simon, E. S., Prime, K. L. & Whitesides, G. M. (1991) *J. Am. Chem. Soc.* **113,** 12–20.
18. Prime, K. L. & Whitesides, G. M. (1993) *J. Am. Chem. Soc.* **115,** 10714–10721.
19. Wang, R. L. C., Kreuzer, H. J. & Grunze, M. (1997) *J. Phys. Chem. B* **101,** 9767–9773.
20. Harder, P., Grunze, M., Dahint, R., Whitesides, G. M. & Laibinis, P. E. (1998) *J. Phys. Chem. B* **102,** 426–436.
21. Feldman, K., Hähner, G., Spencer, N. D., Harder, P. & Grunze, M. (1999) *J. Am. Chem. Soc.* **121,** 10134–10141.
22. Kenausis, G. L., Vörös, J., Elbert, D. L., Huang, N., Hofer, R., Ruiz-Taylor, L., Textor, M., Hubbell, J. A. & Spencer, N. D. (2000) *J. Phys. Chem. B* **104,** 3298–3309.
23. Park, K. D. & Kim, S. W. (1992) in *Poly(Ethylene Glycol) Chemistry: Biotechnical and Biomedical Applications*, ed. Harris, J. M. (Plenum, New York), pp. 283–301.
24. Elbert, D. L. & Hubbell, J. A. (1998) *Chem. Biol.* **5,** 177–183.
25. Green, N. M. (1970) *Methods Enzymol.* **18,** 418–424.
26. Larson, P. E. & Kelly, M. A. (1998) *J. Vacuum Sci. Technol. A* **16,** 3483–3489.
27. Physical Electronics (1999) *Sensitivity Factors Database*, MULTIPACK (Physical Electronics, Eden Prairie, MN), Version 6.1A.
28. Reilman, R. F., Msezane, A. & Manson, S. T. (1976) *J. Electron Spectrosc. Related Phenomena* **8,** 389–394.
29. Briggs, D. & Seah, M. P., eds. (1990) *Practical Surface Analysis by Auger and X-Ray Photoelectron Spectroscopy* (Wiley, Chichester, U.K.).
30. Delamarche, E., Bernard, A., Schmid, H., Bietsch, A., Michel, B. & Biebuck, H. (1998) *J. Am. Chem. Soc.* **120,** 500–508.
31. Green, N. M. (1990) *Methods Enzymol.* **184,** 51–67.